Supporting Information

Residue-Specific Interactions of an Intrinsically Disordered Protein with Silica Nanoparticles and Their Quantitative Prediction

Mouzhe Xie,[1] Alexandar L. Hansen,[2] Jiaqi Yuan,[1] and Rafael Brüschweiler[1,2,3*]

[1]Department of Chemistry and Biochemistry, The Ohio State University, Columbus, Ohio 43210, United States

[2]Campus Chemical Instrument Center, The Ohio State University, Columbus, Ohio 43210, United States

[3]Department of Biological Chemistry and Pharmacology, The Ohio State University, Columbus, Ohio 43210, United States

[*]To whom correspondence should be addressed:

Rafael Brüschweiler, Ph.D.

CBEC Building, Department of Chemistry and Biochemistry, The Ohio State University, Columbus, Ohio 43210

E-mail: bruschweiler.1@osu.edu

Tel. 614-688-2083

MATERIALS AND METHODS

Expression and Purification of ^{15}N-Labeled WT p53TAD and Its Mutants

The DNA fragment corresponding to WT p53TAD (1-73 residues) was amplified with polymerase chain reaction and was cloned into a pTBSG ligation independent cloning vector derivative.[1] The DNA fragments of K24N and F19A/W23A mutants of p53TAD were generated using the QuikChange Lightening site-directed mutagenesis protocol (Agilent Technologies) with forward mutagenic primers 125 ng each, and processed in the same way to get plasmids, which were validated by sequencing (GENEWIZ Inc.). For either p53TAD or its mutants, the corresponding plasmid was transformed into *Escherichia coli* BL21(DE3) strain and allowed to grow on an ampicillin-doped LB agar plate. A fresh colony was then inoculated overnight at 37°C in 50 mL LB media that contains 100 mg/L ampicillin, and the cell suspension was centrifuged at 4,000 rpm for 20 min to get cell pellet, which was then transferred into 1 L M9 minimal media containing 1 g $^{15}NH_4Cl$ and 5 g D-glucose (or 4 g D-glucose-$^{13}C_6$ for double-isotopic-labeled sample) to grow. The temperature was maintained at 37°C with a shaking speed of 250 rpm. Once OD_{600} reached 0.75, 1 mM isopropyl β-D-1-thiogalactopyranoside (IPTG) was added into the cell culture to initiate protein expression. The cells were harvested after 4 h and centrifuged at 4,000 rpm, 4°C, for 20 min and washed with 50 mM Tris buffer (pH 7.5, containing 150 mM NaCl and 2 mM EDTA) once, then resuspended in 50 mM sodium phosphate buffer (pH 7.0, containg 500 mM NaCl, 5 mM imidazole, and 20 mM β-mercaptoethanol; ≥7.5 units/mL DNase I (Thermal Scientific) was also added) before being homogenized by EmulsiFlex-C5 (AVESTIN, Inc.). The cell lysate was loaded onto 3 mL Ni-NTA agarose (QIAGEN GmbH) affinity column, washed with 80 mL 25 mM imidazole/phosphate buffer, and eluted with 15 mL 250 mM imidazole/phosphate buffer. The eluate primarily contains target protein with His_6-tag. Tobacco etch virus (TEV) protease, which was also engineered to carry a His_6-tag, was mixed with the eluate by approximately 10 : 1 (His_6-protein : protease) ratio in a 1 kD cut-off dialysis bag (Spectrum Laboratories, Inc.) and extensively dialyzed in 2 L of 50 mM sodium phosphate buffer (pH 7.0, 500 mM NaCl, 20 mM β-mercaptoethanol) for 16 h. A fresh Ni-NTA agarose affinity column was again

used to purify the resulting TEV-cleaved protein. Finally, SDS-PAGE gel electrophoresis was employed to test the expression and purification quality. All the common reagents were purchased from Sigma-Aldrich unless otherwise specified.

NMR Sample Preparation

A. Protein samples. WT p53TAD and its mutants (K24N and F19A/W23A) were exchanged into 50 mM HEPES buffer (pH 7.0, 90% H_2O/10% D_2O) that contains 100 mM NaCl and concentrated to final concentration of 300 μM for relaxation experiments, using Amicon Ultra 4 mL centrifugal filter units (EMD Millipore).

B. Amino acid samples. Twenty common amino acids (natural ^{13}C abundance, L-form except glycine) were purchased from Sigma-Aldrich (His and Tyr) and Fisher Scientific (all others). To prepare the NMR samples, each amino acid (except Tyr) was first dissolved in D_2O (99.9%) by vortexing and sonication, followed by mixing with sodium phosphate buffer and NaCl solution that were also prepared in D_2O to achieve a final solution with 16 mM amino acid, 20 mM sodium phosphate buffer (pD 7.0), and 100 mM NaCl. For the initial solutions of Asp, Cys, and Arg that were either too acidic or basic, 1 M HCl or NaOH solution were used to adjust the pD before they were mixed with phosphate buffer. For Cys samples, 12 mM β-mercaptoethanol was additionally added to minimize di-sulfide bond formation. Due to the poor solubility, Tyr was prepared by using its 2-fold diluted saturated solution at room temperature. The final concentration of Tyr was approximately 1.3 mM.

C. Silica nanoparticle treatment. Bindzil 2040 SNPs were extensively dialyzed in the same buffer before mixing with amino acids or protein constructs. These amorphous, near-spherical SNPs have a relatively narrow size distribution and are negatively charged at the surface (ζ-potential -23.0 ± 7.4 mV) at neutral pH, as characterized previously.[2] In all SNP-doped samples for relaxation experiments, either 2.5% w/w (2.1 μM) for amino acid samples or 1.3% w/w (1.1 μM) for protein samples SNPs were used unless otherwise specified.

Dynamic Light Scattering and ζ-potential Measurements

Dynamic light scattering (DLS) and ζ-potential measurements were performed at 25 °C using Malvern Zetasizer Nano ZS equipped with 633 nm He-Ne laser and 173° back-scatter detector. SNPs were dialyzed into NMR buffers and diluted to approximately 5 mg/mL. For the p53TAD-present sample, SNPs were mixed with p53TAD (c.a. 1 : 20) and shaked for 2 hours before diluting. DLS data were recorded for 12 scans, analyzed using Malvern Zetasizer Software, and reported as volume distribution.

Relaxation Experiments

^{13}C and ^{15}N spin relaxation experiments were performed on Bruker Avance III HD Ascend 850 MHz spectrometers equipped with TCI cryoprobes. For protein samples, either without or with SNPs, the backbone amide ^{15}N spin relaxation parameters were obtained in a pseudo-3D fashion using conventional R_1 and $R_{1\rho}$ experiments by extracting the 2D peak intensities from ^{1}H-^{15}N cross-peaks of enhanced-HSQC-type experiments recorded with eight delay intervals (R_1 = {0.04, 0.20×2, 0.40, 0.60, 0.80×2, 1.00 s}; $R_{1\rho}^{f}$ = {2, 28×2, 54, 80, 112×2, 148 ms}; $R_{1\rho}^{\mathrm{SNP}}$ = {2, 18×2, 36, 54, 72×2, 96 ms}) at 298 K, followed by fitting the intensity-delay data with a single exponential decay curve. Duplicated delay points (denoted by ×2) were employed to ensure good reproducibility of the experiments and to estimate fitting error. R_2 relaxation rates were thereafter obtained using the equation:

$$R_2 = R_{1\rho} / \sin^2\theta - R_1 / \tan^2\theta \qquad \text{(S1)}$$

where $\theta = \arctan(\nu/\Omega)$ is the tilt angle in the rotating frame. Here, ν denotes ^{15}N spin-lock field strength (Hz), which was set to 2047 Hz and was calibrated as reported previously,[3] and Ω is the resonance offset from the spin-lock carrier (Hz) for each cross-peak. To estimate statistical errors of R_1 and R_2, 200 iterations of Monte Carlo error analysis were used.

The peak assignments of WT p53TAD and F19A/W23A mutant were previously done by Shan *et al.*[4] The peak assignments of K24N mutant were kindly provided by

Prof. G. W. Daughdrill (University of South Florida). The ^{15}N relaxation parameters obtained from the heavily overlapped Try53 and Phe54 ^{1}H-^{15}N cross-peaks as a single cross-peak were used in the subsequent analysis for both residues, whereas the heavily overlapped Val10 and Leu25, Glu17 and Arg65, Ala39 and Ala69, ^{1}H-^{15}N cross-peaks (for K24N only) were omitted.

Similarly, the effective R_1 and R_2 (CPMG) for the 20 amino acids, without or with SNPs, were obtained in a pseudo-2D fashion based on the 1D peak intensities from natural abundance ^{1}Hα-^{13}Cα cross-peaks of enhanced-HSQC-type experiments vs delay intervals. The proton-decoupled CPMG pulse sequence for measuring ^{13}Cα-R_2 relaxation rates were modified from Yuwen *et al.*,[5] with ν_{CPMG} = 109 Hz and *rf* field strength = 3.125 kHz for DIPSI-2 decoupling. It allows a longer observation window (> 500 ms) for R_2 relaxation with better precision compared to conventional $R_{1\rho}$-type of experiments for molecules in the extreme narrowing limit, hence is favorably applicable to amino acids. Due to the large variation in R_2 rates for different amino acids in the presence of SNPs, the delay intervals were adjusted so that the peak intensity corresponding to the longest interval was sufficiently decreased (approximately 2.7-fold less) compared to the peak intensity without any delay. Complete relaxation delay intervals are specified as follows: R_1 = {0.05, 0.20×2, 0.40, 0.80, 1.40×2, 2.00 s}; R_2^f = {0, 147×2, 442, 295, 589×2, 737 ms}; R_2^{SNP} = {0, 18x2, 37×2, 55, 74×2 ms} for Arg, His, Lys, and Pro; {0, 37×2, 74×2, 111, 147×2 ms} for Ile, Met, and Phe; {0, 55×2, 111×2, 166, 221×2 ms} for Trp; {0, 74×2, 147×2, 221, 295×2 ms} for Leu; {0, 111×2, 221×2, 332, 442×2 ms} for Ala, Asn, Gln, and Tyr; {0, 147×2, 295, 442, 589×2, 737 ms} for Asp, Cys, Gly, Glu, Ser, Thr, and Val.

Prediction of R_2^b of a Fully Nanoparticle Bound Molecule

The R_2 relaxation rates of backbone amide ^{15}N and ^{13}Cα atoms that are rigidly anchored on the SNP surface are dominated by dipolar and chemical shielding anisotropy (CSA) relaxation. They follow Redfield theory according to (Ref. [6] and references therein)

$$R_2 = \frac{1}{2} d_{\mathrm{XH}}[4J(0) + 3J(\omega_{\mathrm{X}}) + J(\omega_{\mathrm{H}} - \omega_{\mathrm{X}}) + 6J(\omega_{\mathrm{H}}) + 6J(\omega_{\mathrm{H}} + \omega_{\mathrm{X}})]$$

$$+ \frac{1}{6} c_{\mathrm{XH}} \omega_{\mathrm{X}}^2 [4J(0) + 3J(\omega_{\mathrm{X}})] \tag{S2}$$

where X stands for either ^{13}C or ^{15}N spins, $d_{\mathrm{XH}} = (1/20)(\mu_0/4\pi)^2 (h/2\pi)^2 \gamma_{\mathrm{X}}^2 \gamma_{\mathrm{H}}^2 \left\langle r_{\mathrm{XH}}^{-3} \right\rangle^2$, and $c_{\mathrm{XH}} = (1/15)\Delta\sigma^2$. μ_0 is the permeability of vacuum, h is Planck's constant, γ_{H} and γ_{X} are the gyromagnetic ratios of the corresponding nuclei, and the backbone C-H or N-H bond lengths are r_{CH} = 1.10 Å and r_{NH} = 1.02 Å, respectively. The chemical shielding anisotropy (CSA), $\Delta\sigma$, has been set to 25 ppm for ^{13}Cα[7] and -170 ppm for ^{15}N.[8] $J(\omega)$ is the spectral density function, which is expressed as

$$J(\omega) = \frac{2\tau_{\mathrm{c}}}{1 + \omega^2 \tau_{\mathrm{c}}^2} \tag{S3}$$

where ω is the angular frequency (in rad/s) of relevant spin transitions and τ_{c} is the rotational correlation time of the molecule or nanoparticle, which can be estimated from the Stokes-Einstein-Debye relationship:

$$\tau_{\mathrm{c}} = \frac{V\eta}{k_{\mathrm{B}}T} \tag{S4}$$

where $V = 4\pi/(3r^3)$ is the hydrodynamic volume of a single nanoparticle, η is the shear viscosity of the solvent, k_{B} is the Boltzmann constant, and T is the absolute temperature.

Using the parameters r_{SNP} = 10 nm, T = 298 K, η = 0.890 mPa·s, R_2^b of the SNP-bound state was estimated as R_2^b (^{15}N) = 1.6 × 10^3 s^{-1} and R_2^b (^{13}Cα) = 3.8 × 10^3 s^{-1} for the estimation of average SNP-bound population of WT p53TAD $\langle p_b \rangle$ = 0.28% (Eq. (2)). Predicted R_1^b (^{15}N) equals 0.01 s^{-1}, using the following expression:

$$R_1 = d_{\mathrm{XH}}[3J(\omega_{\mathrm{X}}) + J(\omega_{\mathrm{H}} - \omega_{\mathrm{X}}) + 6J(\omega_{\mathrm{H}} + \omega_{\mathrm{X}})] + c_{\mathrm{XH}} \omega_{\mathrm{X}}^2 J(\omega_{\mathrm{X}}) \tag{S5}$$

Numerical Values of Model Parameters of Free Residue Interaction Model (FRIM)

The numerical values used in the FRIM model of Eq. (5):

$$p_i^b = \frac{\Delta R_{2,i}}{R_2^b} = \frac{1}{R_2^b}\sum_j A_j \exp\{-|i-j|/\lambda_j\}$$

- *Positively charged residues, including the N-terminal NH_3^+-group,* were treated according to Eq. (4). The affinity value A_j^{positive} was set to 4.1 and the interaction range was set to $\lambda_j^{\text{positive}}$ = 14.0 residues whereby $\lambda_{\text{N-term}}$ = 7.0 residues (half of 14.0) for the N-terminal NH_3^+-group. A_j^{positive} = 4.1 and $\lambda_j^{\text{positive}}$ = 14.0 residues was directly obtained from $\Delta\Delta R_2$ profiles of WT vs. K24N mutant (Figure 2c and Eq. (4)). In the K24N mutant, the positive Lys with its strong attractive interaction was replaced by Asn, which has minimal affinity to SNPs (Figure 3). This property allowed us to experimentally isolate the effect of Lys on SNP binding (Figure 2c).
- *For the negatively charged residues Glu and Asp*, A_j was set to a fitted negative value A_j^{negative} = -1.0 s^{-1}, which takes into account electrostatic repulsion exerted by the anionic SNPs, and their interaction range was set to A_j^{negative} = 6.4 residues whereby $\lambda_{\text{C-term}}$ = 3.2 residues (half of 6.4) for the C-terminal COO^--group.
- *All other residues, which are neutral:* A_j^{neutral} was scaled proportionally (scaling factor 0.155) to the amino-acid specific SNP affinity of residue *j* given in Figure 3 and Table S1 with a uniform interaction range $\lambda_j^{\text{neutral}}$ = 2.8 residues.
- The total number of fitting parameters is 4, namely (1) the negative affinity of negatively charged residues A_j^{negative} = -1.0 s^{-1}, (2) the persistence length of negatively charged residues $\lambda_j^{\text{negative}}$ = 6.4 residues, (3) the persistence length of neutral residues $\lambda_j^{\text{neutral}}$ = 2.8 residues, and (4) an overall scaling factor 0.155 to the experimentally derived affinity of neutral residues.

- The *de novo* FRIM fitting parameters for WT p53TAD is provided in Table S2 as an example.

Estimation of SNP Particle Concentration

The weight percentage w of silica in SNP stock colloid (Bindzil 2040, Eka Chemicals) was quantified to be (33.80 ± 0.01)% by gravimetric analysis after complete solvent evaporation at 95°C for 48 h. Density of the colloid ρ_0 was determined to be 1.29 ± 0.01 g/mL. The average diameter (19.5 ± 5.3 nm) of SNPs was estimated from transmission electron microscopy (TEM) as described previously.[2] In short, all of the discernable nanoparticles (approximately 200 in total, each counted twice from two orthogonal axes) in selected confined regions from three TEM images were analyzed to obtain size distribution. Dynamic light scattering analysis confirmed the monodispersity of the SNPs in NMR buffer conditions.

Taking r = 10 nm as an average radius and assuming all nanoparticles have spherical morphology, each nanoparticle has a volume of $V_{\mathrm{p}} = \frac{4}{3}\pi r^3 = 3.9 \times 10^3\,\mathrm{nm}^3$, and thus a mass of $m_{\mathrm{p}} = 8.6 \times 10^{-18}$ g, where the density of amorphous silica $\rho(SiO_2) = 2.196$ g/cm^3 was used (CRC Handbook of Chemistry and Physics, 96th ed. 2015-2016). Therefore, the particle concentration n of SNP stock colloid could be estimated according to the following equation:

$$n = \frac{W}{m_{\mathrm{p}} N_{\mathrm{A}}} = \frac{w\rho_0}{m_{\mathrm{p}} N_{\mathrm{A}}} \cong 84\ \mu\mathrm{M} \qquad \text{(S6)}$$

where $W = w\rho_0$ is the mass concentration (in g/mL) of silica in the stock colloid and N_{A} is the Avogadro constant. This value was used to estimate the particle concentration of SNPs for samples used in the current study.

Table S1. Experimental $^{13}C\alpha$ relaxation parameters, in the absence or presence of SNPs, and the derived affinity scale for all 20 amino acids (see Figures 3 and S1 for visualization). For free amino acids, the variation in R_1 and R_2 rates results from the differences in molecular size. Larger molecules (such as Trp, Tyr, Arg, Phe, His, and Lys) tumble more slowly with larger τ_c values, resulting in larger R_1 and R_2 values. Note that all amino acids tumble sufficiently rapidly and therefore are in the extreme narrowing regime, where R_1 or R_2 are relatively close to each other. In the presence of SNPs, R_1 changes only little while R_2 varies quite dramatically for several amino acids.

Amino acid	SNP-free, $^{13}C\alpha$ (s^{-1})				SNP (2.5% w/w)-present, $^{13}C\alpha$ (s^{-1})				ΔR_2 (s^{-1})	A_j (s^{-1})
	R_1	R_1 error	R_2	R_2 error	R_1	R_1 error	R_2	R_2 error		
Ala	0.23	0.02	0.53	0.04	0.25	0.03	1.25	0.06	0.72	0.72
Arg	0.61	0.02	1.06	0.04	0.83	0.03	22.15	0.83	21.09	4.09 [a]
Asn	0.36	0.01	0.70	0.03	0.38	0.03	1.22	0.04	0.52	0.52
Asp	0.37	0.02	0.71	0.03	0.35	0.03	0.95	0.03	0.24	-1.02 [b]
Cys	0.26	0.02	1.35	0.04	0.45	0.04	2.55	0.06	1.20	1.20 [c]
Gln	0.45	0.02	0.75	0.03	0.47	0.02	1.37	0.05	0.62	0.62
Glu	0.47	0.02	0.80	0.03	0.47	0.02	1.09	0.03	0.29	-1.02 [b]
Gly	0.27	0.01	0.52	0.03	0.42	0.02	0.95	0.03	0.43	0.43
His	0.52	0.01	1.00	0.02	0.62	0.02	10.84	0.34	9.84	9.84 [c]
Ile	0.44	0.01	0.81	0.02	0.49	0.03	10.84	0.35	10.03	10.03
Leu	0.42	0.01	0.75	0.03	0.49	0.02	10.14	0.28	9.39	9.39
Lys	0.57	0.02	0.91	0.03	0.73	0.02	13.59	0.32	12.68	4.09 [a]
Met	0.43	0.02	0.74	0.03	0.50	0.02	5.26	0.19	4.52	4.52
Phe	0.56	0.01	0.90	0.01	0.61	0.03	8.78	0.29	7.88	7.88
Pro	0.20	0.02	0.43	0.02	0.30	0.02	14.64	0.65	14.21	14.21
Ser	0.30	0.01	0.55	0.03	0.33	0.01	0.86	0.03	0.31	0.31
Thr	0.37	0.01	1.01	0.03	0.43	0.02	1.45	0.04	0.44	0.44
Trp	0.74	0.02	1.14	0.03	0.77	0.02	4.81	0.11	3.67	3.67
Tyr	0.79	0.05	1.17	0.08	0.75	0.05	2.47	0.15	1.30	1.30 [c]
Val	0.35	0.01	0.80	0.03	0.40	0.02	6.48	0.19	5.68	5.68

[a] Experimentally obtained absolute value, no overall scaling factor was used in FRIM for back-calculation. [b] Fitted absolute value, no overall scaling factor was used in FRIM for back-calculation. [c] Value not used in FRIM in this study, due to the absence of corresponding amino acid residue in protein constructs' primary sequence.

Table S2. *De novo* fitting parameters of FRIM (Eq. (5)) and its application to WT p53TAD. See Figure S2 for a graphical display of the amino-acid specific A_j parameters.

Sequence	A_j (s^{-1})	λ_j †	^{15}N-ΔR_2 (s^{-1})		Sequence	A_j (s^{-1})	λ_j †	^{15}N-ΔR_2 (s^{-1})	
			FRIM	Expt.				FRIM	Expt.
N-term -NH_3^+	4.09	7.0	4.02	--	P36	2.20	2.8	6.33	--
N-term S	0.05	2.8	3.54	--	S37	0.05	2.8	4.85	5.66
N-term N	0.08	2.8	3.17	--	Q38	0.10	2.8	3.85	4.39
N-term A	0.11	2.8	2.89	--	A39	0.11	2.8	3.20	2.92
M1	0.70	2.8	2.74	1.83	M40	0.70	2.8	2.82	2.97
E2	-1.02	6.4	2.31	2.24	D41	-1.02	6.4	2.30	2.77
E3	-1.02	6.4	2.46	2.48	D42	-1.02	6.4	2.43	2.49
P4	2.20	2.8	3.24	--	L43	1.46	2.8	3.23	2.92
Q5	0.10	2.8	2.84	2.62	M44	0.70	2.8	3.44	3.00
S6	0.05	2.8	2.74	2.60	L45	1.46	2.8	3.62	3.08
D7	-1.02	6.4	2.96	2.71	S46	0.05	2.8	3.25	3.26
P8	2.20	2.8	3.92	--	P47	2.20	2.8	3.31	--
S9	0.05	2.8	3.82	3.82	D48	-1.02	6.4	2.27	2.90
V10	0.88	2.8	4.17	4.55	D49	-1.02	6.4	1.94	2.62
E11	-1.02	6.4	4.44	5.14	I50	1.56	2.8	2.28	2.59
P12	2.20	2.8	5.60	--	E51	-1.02	6.4	1.86	2.44
P13	2.20	2.8	5.86	--	Q52	0.10	2.8	2.07	2.33
L14	1.46	2.8	5.24	4.65	W53	0.57	2.8	2.51	2.26
S15	0.05	2.8	4.18	3.50	F54	1.22	2.8	2.84	2.26
Q16	0.10	2.8	3.54	3.35	T55	0.07	2.8	2.64	2.51
E17	-1.02	6.4	3.21	3.46	E56	-1.02	6.4	2.69	2.48
T18	0.07	2.8	3.52	3.82	D57	-1.02	6.4	3.37	3.26
F19	1.22	2.8	4.11	3.93	P58	2.20	2.8	4.73	--
S20	0.05	2.8	4.19	4.31	G59	0.07	2.8	4.97	4.11
D21	-1.02	6.4	4.59	5.63	P60	2.20	2.8	5.62	--
L22	1.46	2.8	5.70	5.97	D61	-1.02	6.4	5.19	4.68
W23	0.57	2.8	6.23	6.64	E62	-1.02	6.4	5.50	4.94
K24	4.09	14.0	6.83	7.09	A63	0.11	2.8	6.52	6.91
L25	1.46	2.8	7.37	7.68	P64	2.20	2.8	7.89	--
L26	1.46	2.8	7.48	4.65	R65	4.09	14.0	8.20	8.18
P27	2.20	2.8	7.18	--	M66	0.70	2.8	8.42	8.72
E28	-1.02	6.4	5.95	6.93	P67	2.20	2.8	8.64	--
N29	0.08	2.8	5.57	5.06	E68	-1.02	6.4	7.80	7.94
N30	0.08	2.8	5.62	4.89	A69	0.11	2.8	7.72	8.44
V31	0.88	2.8	6.11	5.36	A70	0.11	2.8	7.94	9.07
L32	1.46	2.8	6.53	6.41	P71	2.20	2.8	8.47	--
S33	0.05	2.8	6.53	6.39	R72	4.09	14.0	7.83	8.23
P34	2.20	2.8	7.14	--	V73	0.88	2.8	6.93	7.04
L35	1.46	2.8	6.90	6.48	C-term -COO^-	-1.02	3.2	5.64	--

† λ_j indicates the distance in terms of the number of residues along primary sequence.

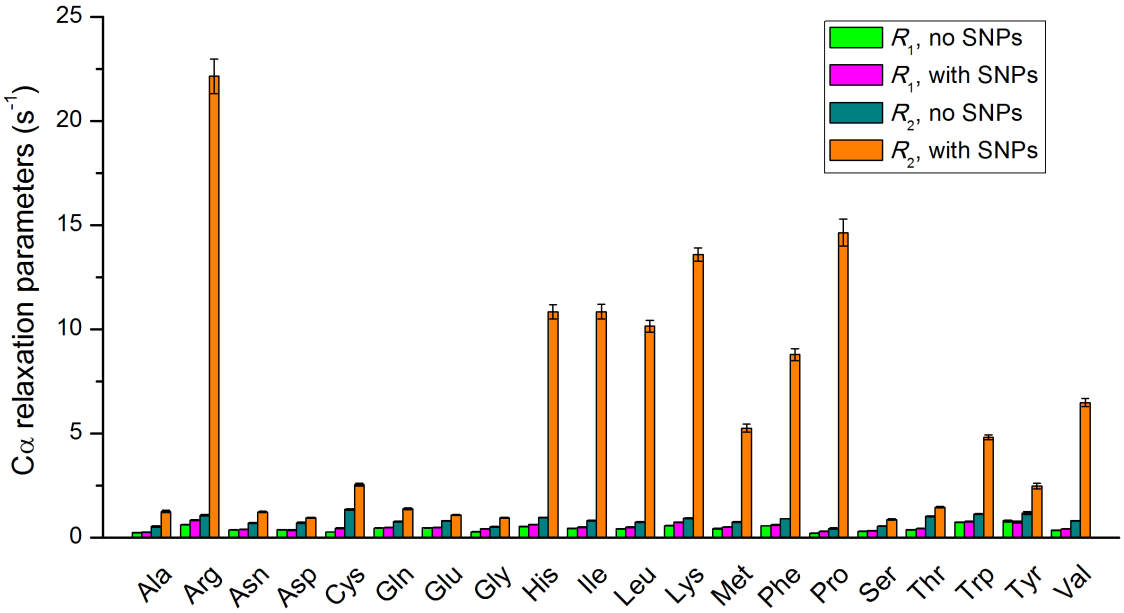

Figure S1. Experimental ^{13}Cα relaxation parameters for all 20 amino acids, in the absence or presence of SNPs (see caption of Table S1 for details).

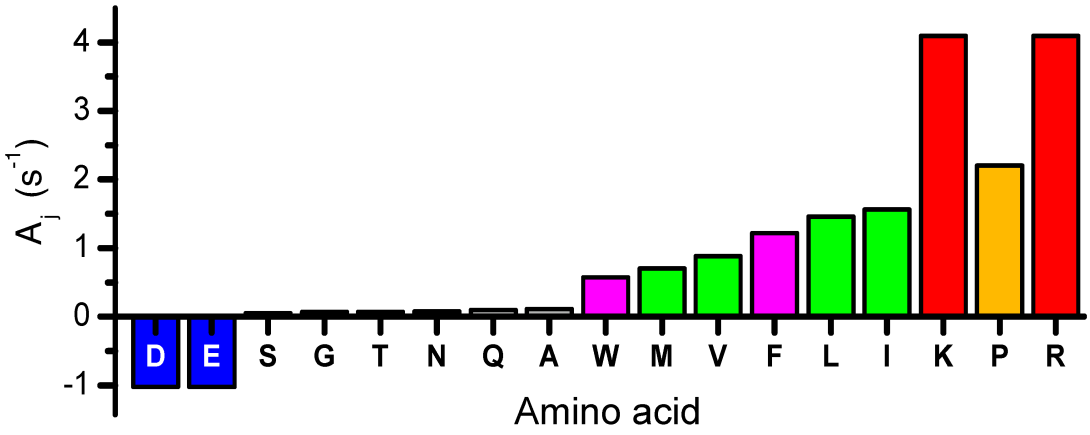

Figure S2. Affinity scale of amino acids used in FRIM to back-calculate $\Delta R_{2,i}$ profiles for WT p53TAD and its mutants. A fixed value 4.1 s^{-1} is determined from Eq. (4) for positively charged residues including Lys and Arg (red). A fitted value -1.0 s^{-1} is used for negatively charged residues, including Asp and Glu (blue), to mimic their repulsive effect to the anionic SNP surfaces. A_j values for all the other amino acids were directly derived from experimentally measured $^{13}C\alpha$-ΔR_2 (Table S1 and Figure 3) by applying a uniform scaling factor 0.155. The amino acids with the largest A_j values, including positively charged residues (red), Proline (orange), methyl-containing residues (green) and aromatic residues (magenta), are color-coded for visualization.

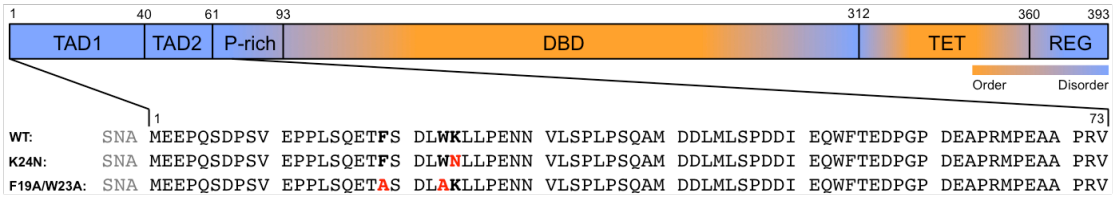

Figure S3. Schematic diagram showing the domain structure of a monomer of human tumor suppressor protein p53, which includes transactivation domains 1 and 2 (TAD1 and TAD2), the proline-rich domain (P-rich), the DNA-binding domain (DBD), the tetramerization domain (TET), and the C-terminal regulatory domain (REG). The approximate intrinsic flexibility of p53 is rendered with colors (orange for structured regions and purple for disordered regions) for visualization. The three constructs used in current study, including wild-type p53TAD and its mutants (K24N and F19A/W23A) are further illustrated with residue sequences, with mutated sites highlighted in bold. Note that three exogenous residues (Ser-Asn-Ala-, shown in gray) are appended at the N-terminus for all constructs after His_6-tag cleavage. The contributions of these residues to the p53TAD-SNP interaction were included in FRIM (Table S2), however, their ^{1}H-^{15}N HSQC cross-peaks are very weak or invisible, prohibiting the accurate measurement of their relaxation parameters.

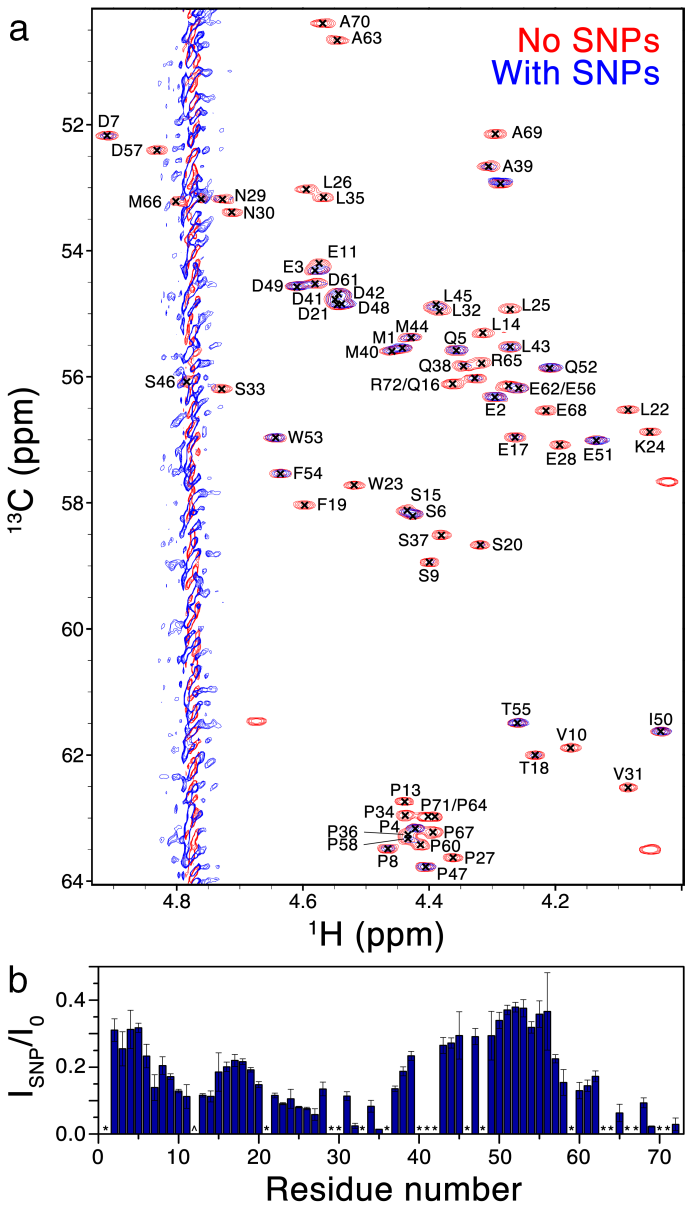

Figure S4. Attenuation of the intensities of ^{1}H-^{13}Cα HSQC cross-peaks of WT p53TAD upon SNP addition. (a) Superimposed spectra of 200 μM ^{15}N,^{13}C-WT p53TAD protein samples in the absence (red) and presence (blue) of 4.7% SNPs by weight. Negative signals are omitted for simplification. The same samples were used to obtain data in Figure 1a,f. (b) Residue-specific intensity ratios (SNP-present over SNP-free) are plotted as bars vs the primary sequence. The overall pattern closely resembles the one observed in ^{1}H-^{15}N HSQC spectra (Figure 1f), indicating that residue-specific interactions of IDPs with nanoparticle can be probed by solution NMR via both backbone ^{13}Cα and ^{15}N spin labels. Intensity of a few cross-peaks (indicated by *) could not be accurately analyzed due to peak overlap, low signal-to-noise, and/or vicinity to the water signal. Pro12 (^), which precedes Pro13, cannot be assigned.

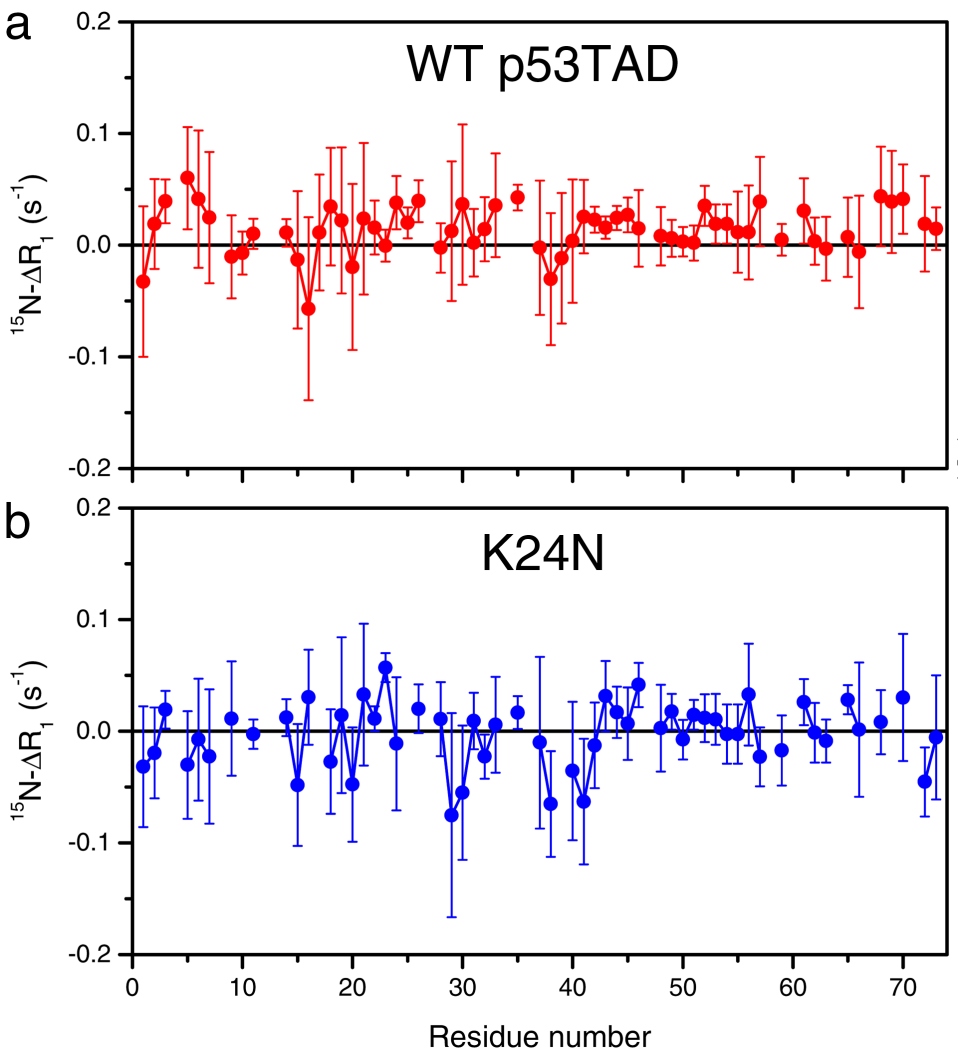

Figure S5. Residue-specific differences of NMR ^{15}N backbone longitudinal relaxation rates of (a) WT p53TAD and (b) K24N in the presence and absence of SNPs, namely $\Delta R_{1,i} = R_{1,i}^{\mathrm{SNP}} - R_{1,i}^{f}$, were plotted along their primary sequences. The consistently small values indicate that R_1 is insensitive to the presence of SNPs, i.e. R_1^b is essentially zero, which is consistent with very slow tumbling of protein when interacting with 20 nm SNPs (see Supporting Information Section "*Prediction of R_2^b of a Fully Nanoparticle Bound Molecule*"). The ΔR_1 behavior is in sharp contrast to the one of ΔR_2 (see Figure 2).

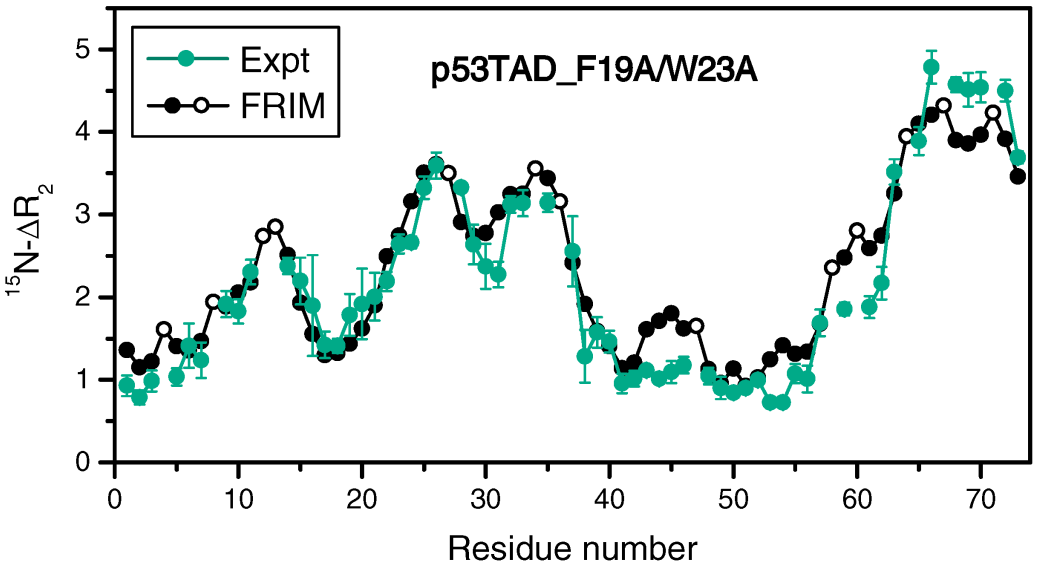

Figure S6. ΔR_2 profiles of 300 μM F19A/W23A mutant of p53TAD in the presence (1.3 μM) and absence of SNPs. The prediction based on FRIM (Eq. (5)) well reproduces the experiment, with a Pearson correlation coefficient r of 0.953, reflecting the absence of long-range interactions of Phe and Trp residues with SNPs. An overall scaling factor of 2.0 was used to correct for the SNP concentration difference compared to the WT p53TAD and K24N samples. Open circles represent Pro residues for which experimental data are not available.

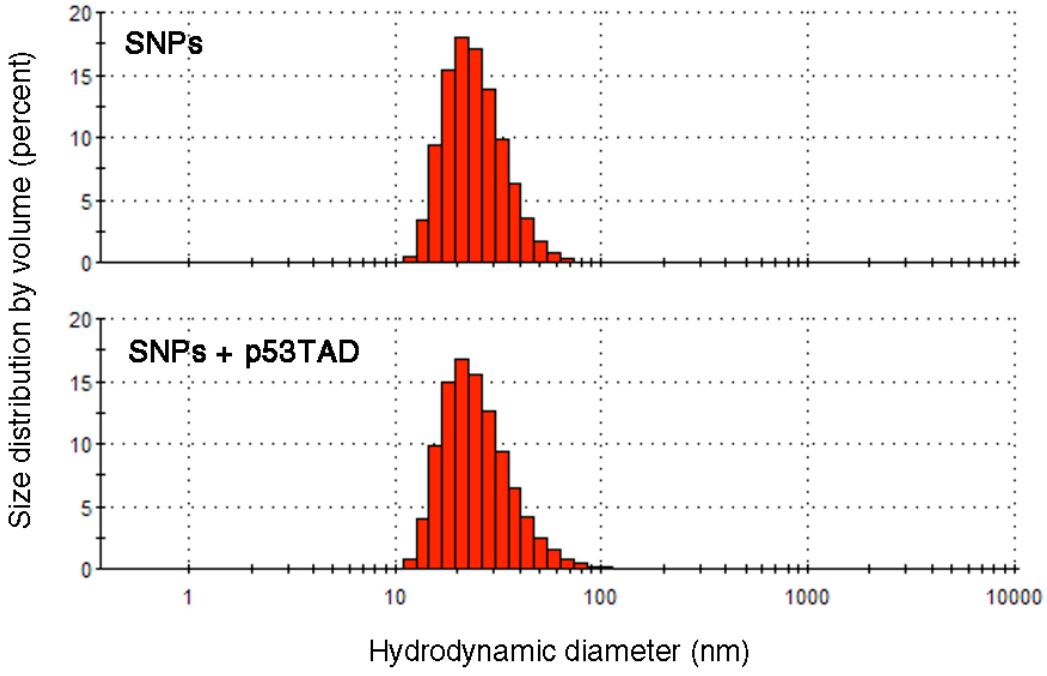

Figure S7. Hydrodynamic size distribution of SNPs without (top) and with (bottom) p53TAD present measured by dynamic light scattering. The two distributions are essentially identical, confirming that the SNPs remain monodispersed in the presence of p53TAD.

REFERENCES

(1) Qin, H.; Hu, J.; Hua, Y.; Challa, S. V.; Cross, T. A.; Gao, F. P. Construction of a Series of Vectors for High Throughput Cloning and Expression Screening of Membrane Proteins from *Mycobacterium tuberculosis*. *BMC Biotechnol.* **2008**, *8*, 1-8.

(2) Zhang, B.; Xie, M.; Bruschweiler-Li, L.; Bingol, K.; Brüschweiler, R. Use of Charged Nanoparticles in NMR-based Metabolomics for Spectral Simplification and Improved Metabolite Identification. *Anal. Chem.* **2015**, *87*, 7211-7217.

(3) Palmer III, A. G.; Kroenke, C. D.; Loria, J. P. Nuclear Magnetic Resonance Methods for Quantifying Microsecond-to-Millisecond Motions in Biological Macromolecules. *Methods Enzymol.* **2001**, *339*, 204-238.

(4) Shan, B.; Li, D.-W.; Bruschweiler-Li, L.; Brüschweiler, R. Competitive Binding between Dynamic p53 Transactivation Subdomains to Human MDM2 Protein: Implications for Regulating the p53·MDM2/MDMX Interaction. *J. Biol. Chem.* **2012**, *287*, 30376-30384.

(5) Yuwen, T.; Skrynnikov, N. R. Proton-Decoupled CPMG: A Better Experiment for Measuring ^{15}N R_2 Relaxation in Disordered Proteins. *J. Magn. Reson.* **2014**, *241*, 155-169.

(6) Gu, Y.; Li, D.-W.; Brüschweiler, R. NMR Order Parameter Determination from Long Molecular Dynamics Trajectories for Objective Comparison with Experiment. *J. Chem. Theory Comput.* **2014**, *10*, 2599-2607.

(7) Wylie, B. J.; Schwieters, C. D.; Oldfield, E.; Rienstra, C. M. Protein Structure Refinement Using ^{13}Cα Chemical Shift Tensors. *J. Am. Chem. Soc.* **2009**, *131*, 985-992.

(8) Tjandra, N.; Szabo, A.; Bax, A. Protein Backbone Dynamics and ^{15}N Chemical Shift Anisotropy from Quantitative Measurement of Relaxation Interference Effects. *J. Am. Chem. Soc.* **1996**, *118*, 6986-6991.